Multi-Mission Satellite Remote Sensing for Spatiotemporal Retrieval of Riverine Water Turbidity in the Chao Phraya River, Thailand

Teerawat Suwanlertcharoen[1*], Siam Lawawirojwong[2] and Kampanat Deeudomchan[3]

[1]Geo-Informatics and Space Technology Development Agency (Public Organization), Bangkok 10210, Thailand

[2]Geo-Informatics and Space Technology Development Agency (Public Organization), Bangkok 10210, Thailand

[3]Geo-Informatics and Space Technology Development Agency (Public Organization), Bangkok 10210, Thailand

[*]teerawat@gistda.or.th

***Abstract*:** *Riverine water turbidity is a key indicator of water quality, influencing light penetration, primary productivity, and the transport of sediments and pollutants, factors that directly affect aquatic ecosystems, public health, and water resource management. Given the dynamic nature of river systems, there is a growing need for accurate and timely methods to monitor turbidity over broad spatial and temporal scales. This study explores the potential of multi-mission satellite remote sensing for spatiotemporal retrieval of turbidity in the Chao Phraya River, a major waterway in Thailand that flows into the Gulf of Thailand. The research integrates multispectral data from Sentinel-2 (A and B), Landsat-8 and Landsat-9, and hyperspectral imagery from the EMIT mission by NASA. In-situ turbidity data from the Metropolitan Waterworks Authority (MWA) were used for algorithm development and validation. Atmospheric correction and sunglint removal were performed using the Dark Spectrum Fitting (DSF) algorithm in the ACOLITE software, chosen for its proven accuracy over inland and turbid waters. Surface reflectance in the red band was analyzed using a piecewise semi-empirical model employing polynomial and linear regression techniques. Validation against in-situ data showed strong agreement (R^2 = 0.901, RMSE = 5.75 NTU, MAE = 4.68 NTU), demonstrating the effectiveness of the retrieval approach. The results reveal distinct spatiotemporal turbidity patterns along the river throughout 2024. This study confirms the robustness of multi-mission satellite remote sensing for turbidity monitoring and offers valuable insights for water quality management. The findings support informed decision-making for environmental protection and sustainable development, particularly given the influence of the river on the coastal ecosystems of the Gulf of Thailand.*

Keywords: Riverine Water Turbidity, ACOLITE, Satellite Remote Sensing, Chao Phraya River, Piecewise Regression

Introduction

Turbidity is a crucial water quality parameter and serves as a proxy for the clarity of water (Borok, 2014). Its primary effect is the attenuation of light, which subsequently limits photosynthetic activity and phytoplankton productivity (Fisher et al., 1987; Bilotta and Brazier, 2008). Turbidity is influenced by a combination of factors, including suspended inorganic matter, fine detrital particles, and phytoplankton (Yuan, 2021). High river water turbidity frequently occurs after heavy rainfall, runoff events, and flooding (Marina et al., 2020). Elevated turbidity in water bodies impairs light transmission and reduces dissolved oxygen levels, which in turn adversely affects aquatic plants and animals (Güttler et al.,

2013). This condition also facilitates the transport of sediments and pollutants, directly impacting aquatic ecosystems, public health, and water resource management.

The Chao Phraya River is a major and vital waterway in Thailand, with its water being used for various activities, including consumption, agriculture, industry, and maintaining downstream ecosystems. Water quality in the river is a significant issue, primarily due to wastewater discharge from communities, agriculture, and industrial factories (Hydro and Agro Informatics Institute, 2012). The impacts on the downstream estuary align with the findings of Suwanlertcharoen et al. (2024), which demonstrated high nearshore turbidity. Therefore, continuous monitoring of water quality, particularly turbidity, is crucial for managing raw water sources used in tap water production. Monitoring the quality of raw water sources before they enter treatment systems, as well as the downstream areas affected by the transport of freshwater and sediment in the river, is essential. Comprehensive monitoring and early warning systems, spanning from upstream to the sea, are essential for effective water quality management and for protecting activities like coastal and marine aquaculture.

Conventional approaches to water quality monitoring, such as manual field observations and permanent monitoring stations, are often labor-intensive, costly, and limited in their ability to capture comprehensive information. Conventional field-based observations are often irregular in their timing, while permanent stations, though providing more frequent data, are spatially limited. As a result, relying solely on these techniques can lead to a narrow or discontinuous understanding of ecological phenomena over time (Estes et al., 2018). Current remote sensing methods provide the capability to evaluate and monitor water quality indicators, such as suspended sediments, turbidity, chlorophyll-a, and water temperature. These data are crucial for assessing changes in water quality parameters and supporting improved water quality management (Ritchie, Zimba, and Everitt, 2003). Additionally, turbidity can be estimated from remote sensing data based on its optical properties, allowing for extensive spatial and temporal monitoring relative to conventional measurement methods (Shen and Feng, 2018). The use of this method provides a more efficient way to collect data, as it reduces labor and provides current information (Acharya et al., 2018). However, remote sensing imagery is now instrumental in filling both spatial and temporal data gaps, effectively mitigating the limitations of conventional field surveys (Topp et al., 2020). The integration of remote sensing technologies, such as the Sentinel-2 MSI and Landsat 8/9 OLI sensors, has significantly enhanced the ability to retrieve water quality data from smaller water bodies like lakes and rivers. These advancements are

attributed to the sensors' finer spatial (~10–30 m), radiometric, and temporal (5–8 days) resolutions (Cao and Tzortziou 2021; Kuhn et al. 2019; Topp et al. 2020). Recently, The Earth Surface Mineral Dust Source Investigation (EMIT) sensor is a hyperspectral electro-optical instrument which measures the 380–2500 nm range and approximately 60 m ground sampling. EMIT is deployed on the International Space Station and has been operational since July 2022 (Thompson et al., 2024; Shrestha et al., 2024). Several regional studies have used satellite remote sensing to estimate water quality with both semi-analytic (Dogliotti et al., 2015; Liu et al., 2019) and semi-empirical models (Elhag et al., 2019; Vanhellemont, 2019b; Luo et al., 2020; Powers et al., 2023; Kolli and Chinnasamy, 2024). In Thailand, there have also been studies using satellite remote sensing to estimate turbidity in the Chao Phraya River (Suwanlertcharoen et al., 2020; Pimwiset et al., 2022; Virdis et al., 2022).

Atmospheric correction is a critical step in remote sensing, as atmospheric effects significantly reduce the quality of satellite imagery and complicates the accurate analysis of water bodies (Xu et al., 2020). The atmospheric path-radiance in the visible spectrum can be 80–90% higher than the water-leaving radiance, making atmospheric effects a dominant factor in the satellite signal (Gordon, 1985; Warren et al., 2019). Essentially, atmospheric correction methods work by removing atmospheric contributions, such as sunglint and aerosol scattering, from the top-of-atmosphere (TOA) signal (Richter, 1990). Therefore, it is essential to evaluate different atmospheric correction algorithms to improve the accuracy of water quality data retrieval in inland water bodies. Several Several widely accessible atmospheric correction methods exist, including ACOLITE, C2RCC, iCOR, l2gen, Polymer, and Sen2Cor. Among these, the ACOLITE algorithm is particularly effective for eutrophic water bodies, as it estimates atmospheric transmittance and surface reflectance by identifying dark pixels in the imagery (Luo et al., 2020; Ulfa et al., 2020; Vanhellemont and Ruddick, 2018; Vanhellemont, 2019a; Vanhellemont, 2020). The ACOLITE algorithm has proven to be highly successful in a wide range of turbid waters (Pahlevan et al., 2021) and has demonstrated its effectiveness in long-term studies in the river estuary (Wu et al., 2023). Given the dynamic nature of river systems, there is a growing need for accurate and timely methods to monitor turbidity over broad spatial and temporal scales. Multi-mission satellites with multispectral and hyperspectral sensors offer opportunities to enhance the accuracy and frequency of turbidity monitoring. This study explores the potential of multi-mission satellite remote sensing for spatiotemporal turbidity retrieval during year 2024 in the Chao Phraya River, a major waterway in Thailand that flows into the Gulf of Thailand. The research integrates multispectral datasets from Sentinel-2A and Sentinel-2B, Landsat-

8 and Landsat-9, and hyperspectral imagery from the EMIT mission by NASA. In-situ turbidity data from the Metropolitan Waterworks Authority (MWA) were used for algorithm development and validation. Atmospheric correction and sunglint removal were performed using the Dark Spectrum Fitting (DSF) algorithm implemented ACOLITE software, chosen for its proven accuracy over inland and turbid waters.

Methodology

1. Study Area

The Chao Phraya River is a major and vital waterway in Thailand, originating from the confluence of the Ping and Nan rivers in Nakhon Sawan Province. It flows south through the Central Plains and eventually drains into the Gulf of Thailand, and it is one of the country's most significant rivers (Hydro and Agro Informatics Institute, 2012). The region is characterized by a tropical monsoon climate, with the river exhibiting seasonal fluctuations marked by low flows from January to May and peak discharges between September and November (Bidorn et al., 2021). This study focuses on the section of the Chao Phraya River that flows through Bang Pa-in and Bang Sai districts in Phra Nakhon Si Ayutthaya Province, as well as Pathum Thani, Nonthaburi, Bangkok, and Samut Prakan provinces, extending to the river mouth as illustrated in Figure 1.

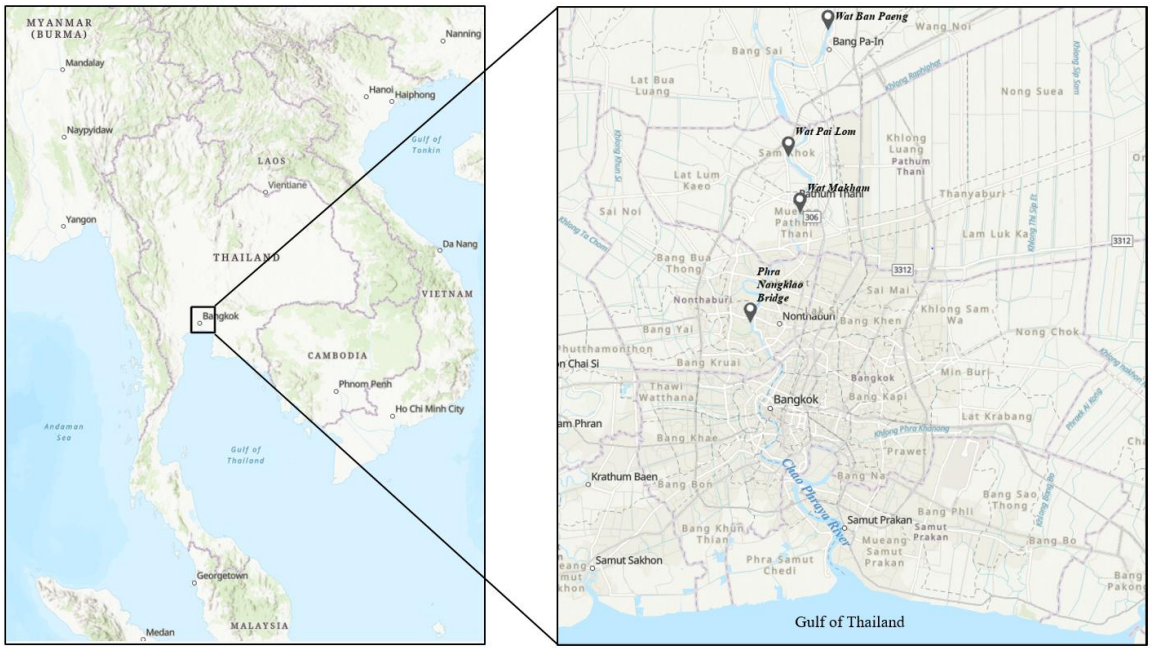

Figure 1: Study area and locations of the MWA automated water quality monitoring stations on the Chao Phraya River.

2. Data Used

2.1 Satellite Imagery

This study utilized satellite remote sensing datasets from 2024, including imagery from Landsat-8 and Landsat-9 OLI, Sentinel-2A and 2B MSI, and EMIT missions. The Sentinel-2 constellation, comprising two polar-orbiting satellites (2A and 2B), is equipped with the Multi-Spectral Instrument (MSI), which captures data across 13 spectral bands spanning the visible, near-infrared, and short-wave infrared regions. The MSI provides spatial resolutions of 10 m, 20 m, and 60 m depending on the spectral band. Sentinel-2 data were obtained as Level-1C products from the Copernicus Data Space Ecosystem (https://browser.dataspace.copernicus.eu/). Each image scene covers a swath width of 290 km, with the two satellites providing a combined revisit interval of five days. Landsat-8 and Landsat-9 Operational Land Imager (OLI) data, offering a spatial resolution of 30 m, were obtained as Level-1 terrain-corrected products (L1TP) from the U.S. Geological Survey (USGS) Earth Explorer platform. These satellites measure in 11 bands, consisting of a coastal aerosol band (430-450 nm), nine visible to shortwave infrared bands (450-2,300 nm), and two thermal bands for the Thermal Infrared Sensor (TIRS) (10,600-12,500 nm). The combined revisiting period for these two satellites is 8 days. NASA's EMIT mission provides hyperspectral imagery, which means it captures data in hundreds of narrow, continuous spectral bands. The EMIT sensor collects data across the visible to shortwave infrared range, specifically from 400 to 2,500 nm, allowing for detailed spectral analysis. For this study, EMIT data collected from January 2023 to April 2025 were used to ensure sufficient information for algorithm development, specifically Level-1B products with a 60 m spatial resolution.

2.2 In-situ Turbidity Data

In-situ turbidity data, measured in Nephelometric Turbidity Units (NTU) and recorded in real-time every 10 minutes, was collected from the MWA automatic water quality monitoring stations on the Chao Phraya River. The data was accessed from MWA's automated water quality monitoring platform, http://rwc.mwa.co.th/page/graph/. For this study, data was selected from four stations—Wat Ban Paeng, Wat Pai Lom, Wat Makham, and Phra Nangklao Bridge—which are located sequentially from upstream to downstream, as shown in Figure 1. These stations were chosen for the completeness and continuity of their data, which covered the year 2024 and corresponded to the satellite imagery used in this study. This in-situ data was used to develop algorithms for estimating water turbidity

from each satellite image and to compare the differences between the actual measured values and the turbidity values derived from the satellite imagery.

3. Methods

The methodological framework and processing workflow adopted in this study are illustrated in Figure 2. Pre-processing of satellite imagery, followed by image analysis for spatiotemporal turbidity assessment, was carried out using the Sentinel Application Platform (SNAP) and Geographic Information System (GIS) tools.

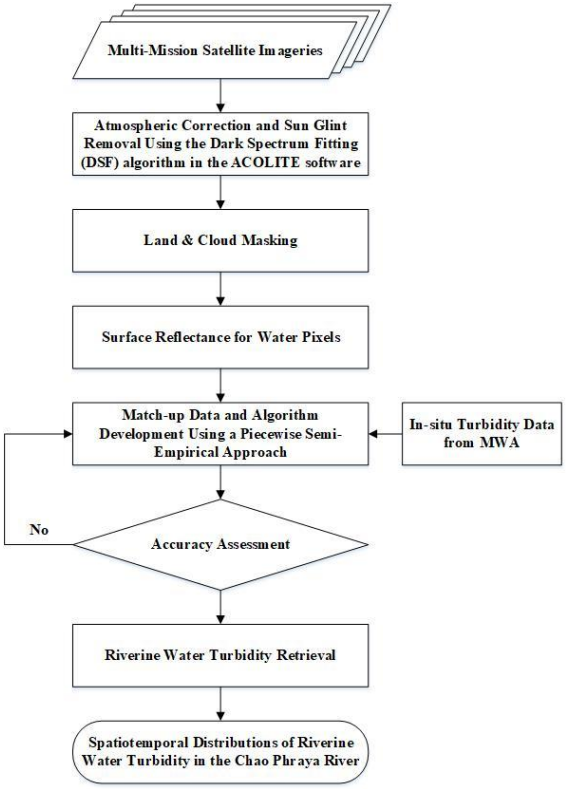

Figure 2: Workflow of the methodology employed in this study.

3.1 Satellite Data Processing

3.1.1 Atmospheric Correction and Sunglint Removal

Atmospheric correction and sunglint removal are crucial steps for converting satellite-measured radiance values into true surface reflectance, a necessary process for accurate water quality analysis (Vanhellemont and Ruddick, 2014). For this study, satellite image pre-processing involved applying the DSF algorithm. DSF, which was developed for meterscale resolution sensors, is integrated into the ACOLITE software (Vanhellemont, 2019a) for atmospheric correction over inland and turbid waters. We used ACOLITE software version 20250402.0 to perform atmospheric correction and sunglint removal on

data from the Sentinel-2 (A and B) MSI, Landsat-8 and Landsat-9 OLI, and EMIT missions. A subsequent step involved land and cloud masking to isolate surface reflectance specifically for water pixels. The process of atmospheric correction in ACOLITE separates the TOA signal observed by a satellite sensor into two distinct components: the atmospheric signal and the surface signal. This is done to accurately retrieve surface reflectances (ρ_s), or water-leaving radiance reflectances (ρ_w), which are the surface-level reflectance for water pixels. This can also be converted to remote sensing reflectance (R_{rs}; unit: sr^{-1}) for water pixels, where $R_{rs} = \rho_w / \pi$. In this study, we used ρ_w to develop an algorithm for turbidity retrieval.

3.1.2 Turbidity Retrieval Algorithm Development

The image processing step involved developing a turbidity retrieval algorithm using a match-up dataset. This dataset compared water-leaving radiance reflectances (ρ_w) from the red band of multi-mission satellite imagery with in-situ turbidity data from MWA automated water quality stations. The data were collected at a time near the acquisition of the satellite imagery. The red band was selected as the primary variable for turbidity analysis due to its strong correlation with the concentration of suspended particles in water. This study employed a piecewise semi-empirical model with two segments separated by a breakpoint. The model combines polynomial and linear regression techniques to quantify turbidity across both low and high ranges, establishing the relationship between red band reflectance and in-situ turbidity data. The piecewise regression model offers flexibility in capturing the non-linear relationships often observed in varying turbidity data.

3.1.3 Spatio-temporal Distribution of Turbidity

Riverine water turbidity was retrieved for each image from the Sentinel-2A and Sentinel-2B MSI, Landsat-8 and Landsat-9 OLI, and EMIT missions during the year 2024. The spatiotemporal distributions of the Chao Phraya River were then analyzed using SNAP and Geographic Information System (GIS) software.

3.2 Evaluation of the Turbidity Retrieval Algorithm

This step included an accuracy assessment where in-situ turbidity data from the MWA automated water quality stations were used for both algorithm development and validation. For algorithm development, the coefficients of a piecewise semi-empirical model were optimized to minimize the the difference between satellite-derived and in-situ turbidity

measurements. Validation was performed during algorithm development to assess the model's performance. The key performance indicators used were:

- Coefficient of Determination (R^2): Indicates how well the model explains the variance in the data.
- Root Mean Square Error (RMSE): Measures the average magnitude of errors between model predictions and in-situ observations.
- Mean Absolute Error (MAE): Measures the average absolute magnitude of errors between model predictions and in-situ observations.

Results and Discussion

1. Algorithm Development and Performance Assessment for Turbidity Retrieval

The characteristics of riverine water turbidity were derived from in-situ data recorded in real-time every 10 minutes throughout 2024 by MWA automatic water quality monitoring stations. These data, as shown in Figure 3, were used for the algorithm's development.

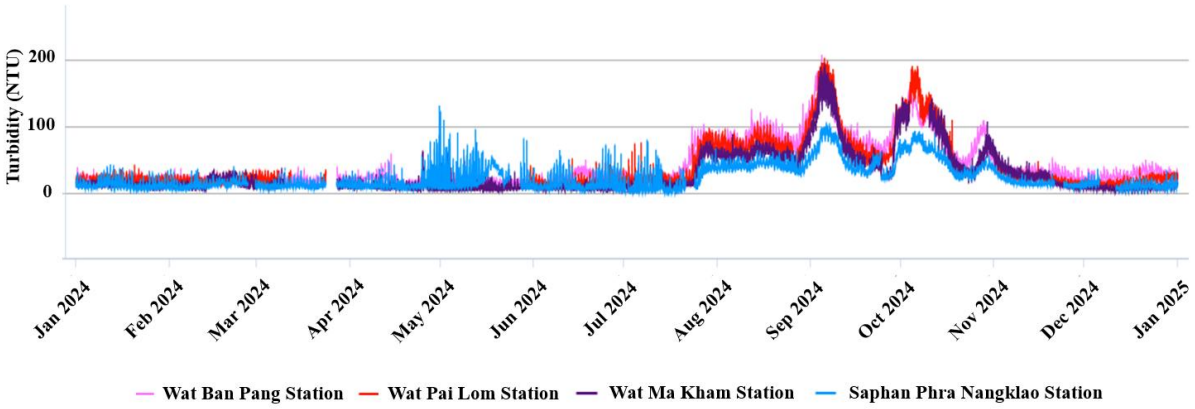

Figure 3: Time series of 10-minute in-situ turbidity data from MWA automatic water quality monitoring stations on the Chao Phraya River, 2024.

In this study, a piecewise semi-empirical model was developed to create an algorithm for estimating water turbidity from multi-mission satellite remote sensing data. This model combines polynomial and linear regression techniques to analyze the relationship between water-leaving radiance reflectances (ρ_w) from various satellite bands and concurrent in-situ turbidity data from automated monitoring stations. The turbidity retrieval algorithm was developed and validated using the red band wavelengths from Sentinel-2A (665 nm), Sentinel-2B (665 nm), Landsat-8 (655 nm), Landsat-9 (654 nm), and EMIT (664 nm) because these bands showed the strongest correlation with measured turbidity values. Analysis revealed a distinct bimodal behavior in the relationship between red band reflectance and in-situ turbidity values. Consequently, a reflectance breakpoint of 0.03 was

established to segment the data, enabling accurate turbidity estimation across both low and high ranges. The final turbidity retrieval algorithm, based on a total of 194 observations, is a piecewise semi-empirical model. It demonstrates a strong relationship between satellite-derived surface reflectance and in-situ turbidity values. This relationship is depicted in Figure 4 and defined by Equations (1) and (2), with specific conditions for the analysis applied as follows:

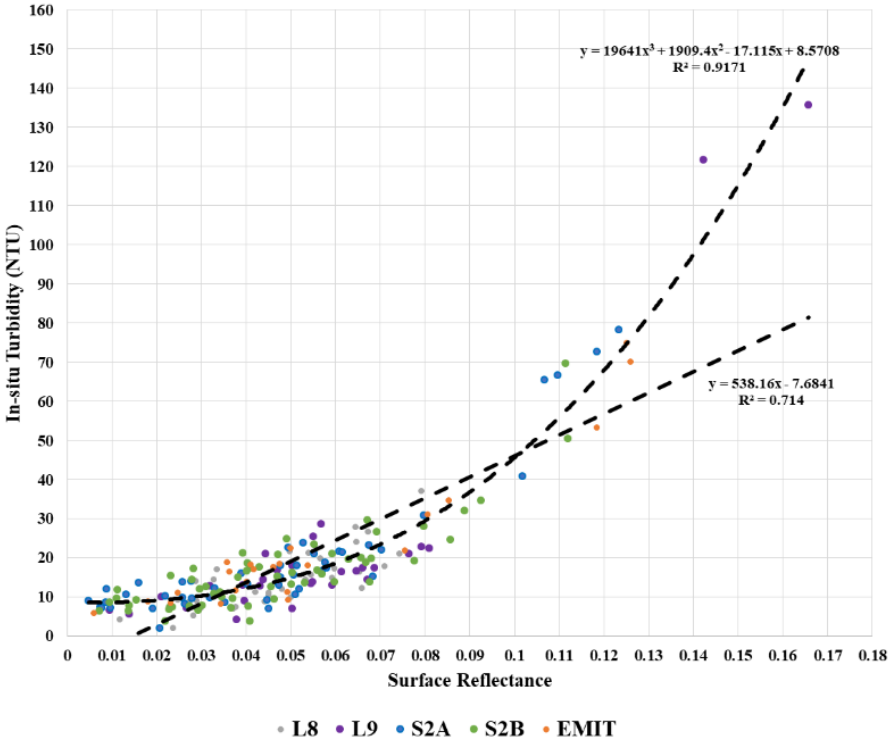

Figure 4: Relationship between satellite-derived water-leaving radiance reflectances (ρ_w) in the red band and in-situ turbidity data.

$$\text{Turbidity (NTU)} = 19{,}641 \cdot \rho_{w,red}^3 + 1{,}909.4 \cdot \rho_{w,red}^2 - 17.115 \cdot \rho_{w,red} + 8.5708 \text{ ; for } \rho_{w,red} \geq 0.03 \quad (1)$$

$$\text{Turbidity (NTU)} = 538.16 \cdot \rho_{w,red} - 7.6841 \text{ ; for } \rho_{w,red} < 0.03 \quad (2)$$

where $\rho_{w,red}$ is the surface-level reflectance for water pixels in the red band wavelength, sourced from multiple satellite missions, including Sentinel-2A (665 nm), Sentinel-2B (665 nm), Landsat-8 (655 nm), Landsat-9 (654 nm), and EMIT (664 nm).

The model's two segments are defined by specific reflectance conditions: Equation (1) applies when the reflectance value (ρ_w) is greater than or equal to 0.03 (R^2 = 0.917), and Equation (2) applies when ρ_w is less than 0.03 (R^2 = 0.714).

Based on the equation, the method was applied to estimate water turbidity from multi-mission satellite imagery and in-situ data. A 1:1 scatter plot of the data distribution (Figure

5) shows a consistent, positive linear relationship. Validation against in-situ data demonstrated strong agreement (R^2 = 0.901, RMSE = 5.75 NTU, MAE = 4.68 NTU), highlighting the effectiveness of the retrieval approach. The development of this water turbidity estimation algorithm is consistent with previous studies. For instance, Vanhellemont (2019a, 2019b) and Luo et al. (2020) also analyzed turbidity retrieval using semi-empirical models with ACOLITE and DSF in turbid water conditions, finding high coefficients of determination. Similarly, Allam et al. (2023) compared atmospheric correction algorithms over inland waters, concluding that ACOLITE performed better in meso- and hypereutrophic waters. Furthermore, the study by Wang et al. (2024) revealed ACOLITE's superior performance in the red band of Sentinel-2 MSI data. This is consistent with the findings of the present study, where ACOLITE with DSF was effective for the Chao Phraya River. The river has an average turbidity of over 10 NTU throughout most of the year, with values potentially exceeding 200 NTU during the flood season. This method performs well in relatively turbid water but has a limitation for $\rho_{w,red}$ values less than approximately 0.03 (below 10 NTU), which may make it less suitable for very clear water. For study areas with clear water, such as oceans or lakes with low turbidity, considering other atmospheric correction methods might be more appropriate.

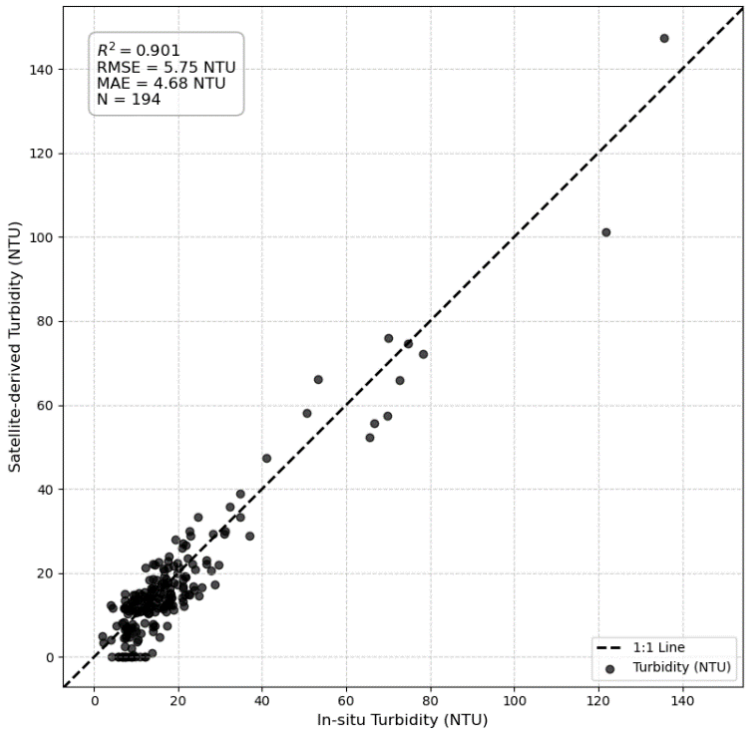

Figure 5: Scatter plot of satellite-derived turbidity versus in-situ turbidity data.

2. Spatio-temporal Distribution of Turbidity

The spatio-temporal distribution of turbidity in the Chao Phraya River, as derived from multi-mission satellite imagery and datasets throughout 2024, was analyzed using Equations 1 and 2, with the results presented in Figure 6. The turbidity values in the river and at its estuary were lower during the dry season (November–April) compared to the flood season (May–October). This is because the dry season has a lower rate of water flow and sediment transport, resulting in lower turbidity. Conversely, after periods of rainfall, the high rate of water flow and sediment transport leads to significantly higher turbidity.

A detailed analysis of multi-temporal turbidity values from 2024 satellite imagery, captured at different sections of the Chao Phraya River near monitoring stations (Figure 7), indicates that average turbidity values began to increase in August, peaking in September, which matches the river discharge peak of that month. The average turbidity was highest in the section of the river near the Wat Ban Paeng Station, followed by the sections near the Wat Pai Lom, Wat Makham, and Phra Nangklao Bridge stations, respectively.

The Chao Phraya River is a crucial source of raw water for the MWA, drawing water at the Sam Lae Pumping Station for its water treatment plants. Therefore, monitoring and analyzing water turbidity before it enters the treatment system is essential. The satellite-derived turbidity analysis in the sections near the Wat Ban Paeng and Wat Pai Lom stations, which are upstream of the Sam Lae Pumping Station, provides a valuable spatial overview of the raw water quality before it reaches the pumping station at different times of the year. During the flood season, water quality problems with high turbidity, often exceeding 100 NTU, are common, whereas turbidity is low during the dry season.

Consequently, multi-temporal monitoring and analysis of water turbidity using satellite imagery are crucial. High turbidity in the raw water source, especially during the flood season, can lead to increased operational and maintenance costs for water treatment (Borok, 2014). For downstream areas, including the estuary of the Chao Phraya River and coastal zones, the water quality is vital for maintaining downstream ecosystems and aquaculture. These areas are also susceptible to the impact of freshwater and sediment plumes. As water turbidity can determine the productivity of a water source, understanding changes in turbidity as the river flows to the sea allows for the prediction of affected areas and the timely issuance of warnings to relevant agencies or aquaculture operators. Therefore, continuous monitoring and surveillance of multi-temporal turbidity values are essential for assessing the current status of the water source and forecasting potential future impacts, leading to more effective planning and mitigation measures for water quality issues that could affect various uses of surface water resources.

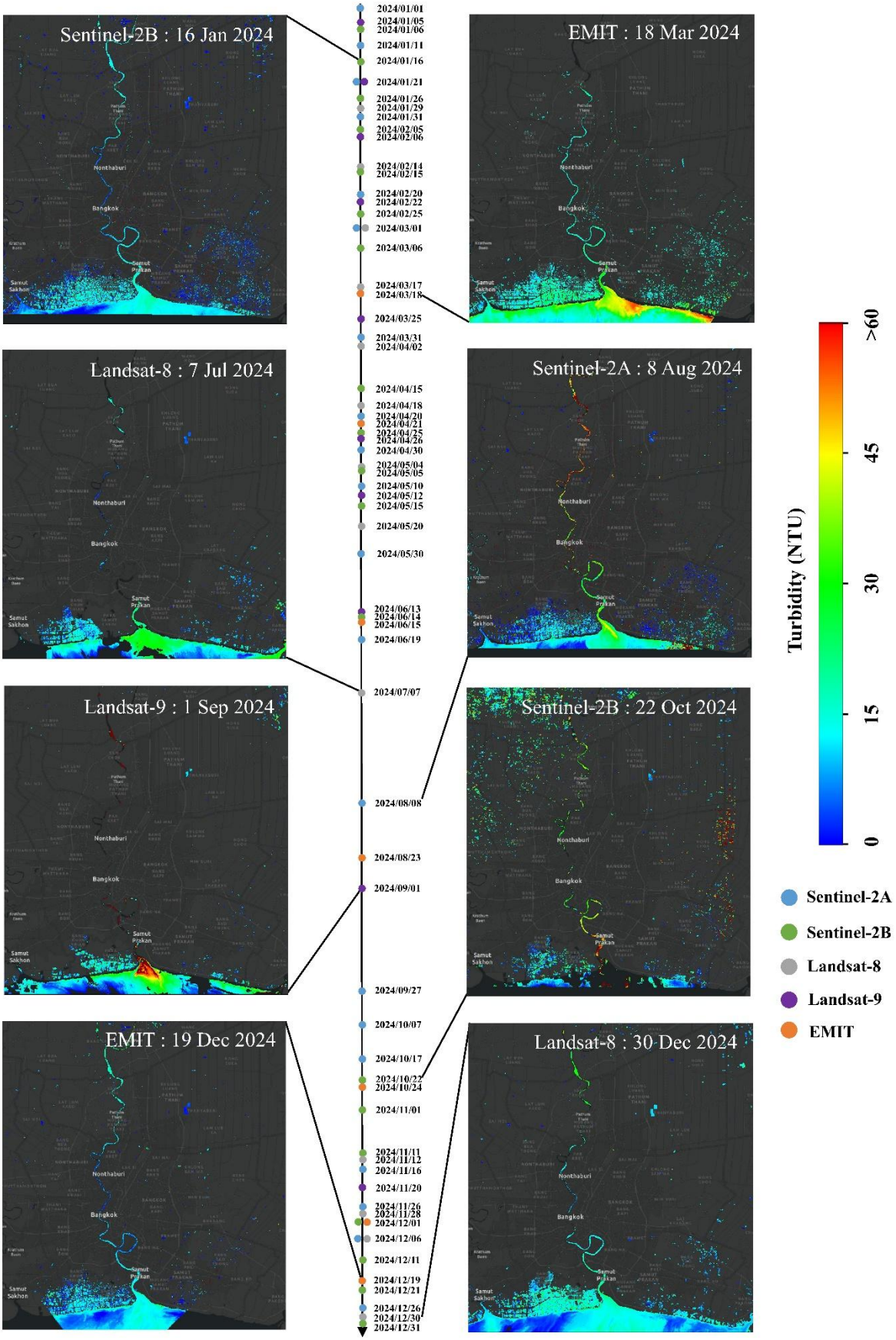

Figure 6: Spatio-temporal distribution of turbidity derived from multi-mission satellite remote sensing imagery and datasets used throughout 2024.

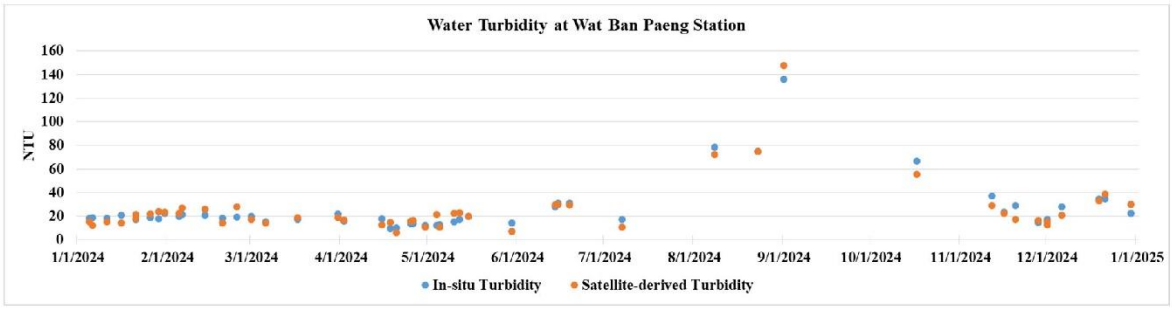

a)

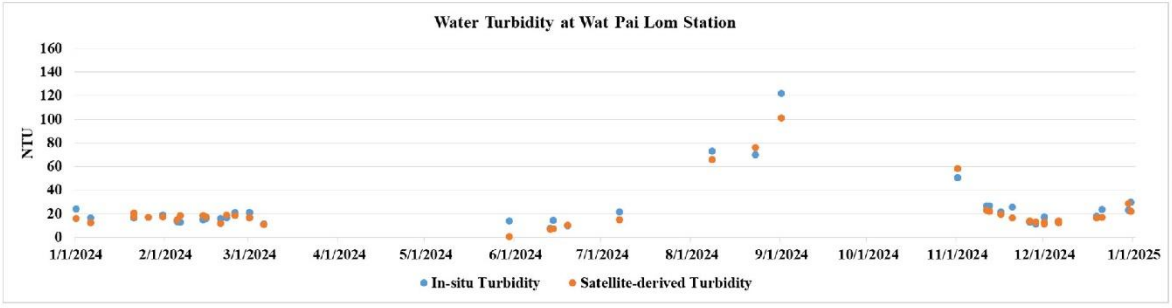

b)

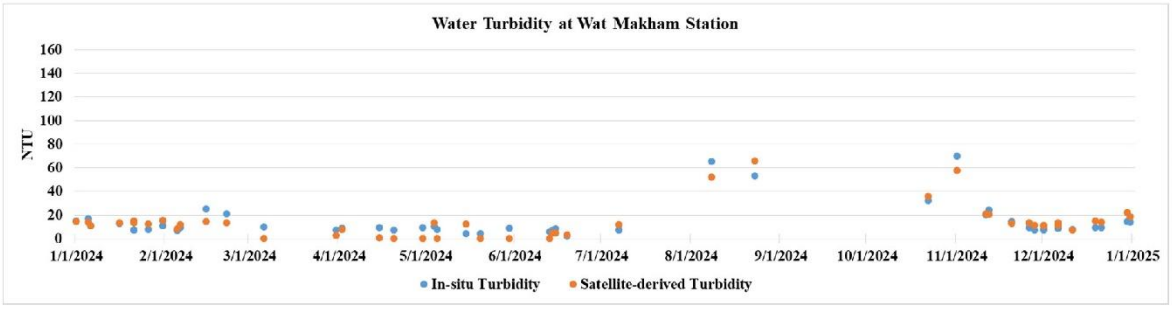

c)

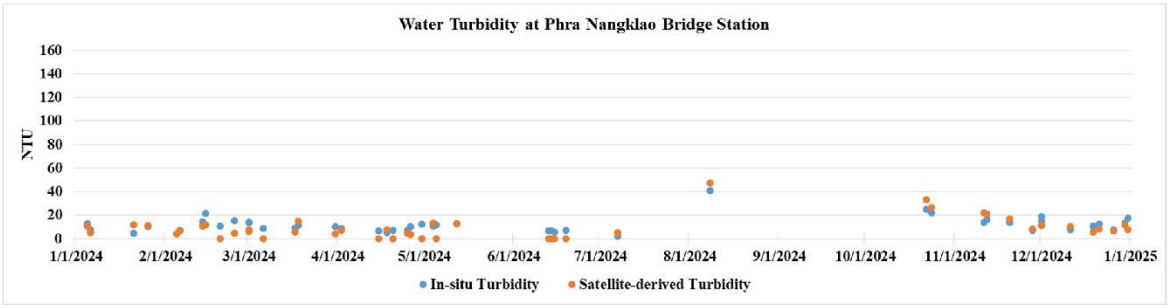

d)

Figure 7: Time series analysis of turbidity derived from satellite imagery and in-situ data from MWA automatic water quality monitoring stations throughout 2024 at Wat Ban Paeng Station (a), Wat Pai Lom Station (b), Wat Makham Station (c), and Phra Nangklao Bridge Station (d).

4. Conclusion and Recommendation

This study successfully demonstrated the effectiveness of using multi-mission satellite remote sensing to retrieve and monitor riverine water turbidity in the Chao Phraya River, Thailand, for the year 2024. The integration of multispectral data from Sentinel-2 (A and

B), Landsat-8 and Landsat-9, and hyperspectral imagery from the EMIT mission, provided a robust approach for spatiotemporal turbidity retrieval.

A key aspect of this research was use of the DSF algorithm within the ACOLITE software for atmospheric correction and sunglint removal. This method proved to be highly accurate for the turbid waters of the Chao Phraya River, as evidenced by a strong validation against in-situ data from MWA automatic water quality monitoring stations (R^2 = 0.901, RMSE = 5.75 NTU, MAE = 4.68 NTU). The developed piecewise semi-empirical model, which uses a combination of polynomial and linear regression based on surface reflectance in the red band, effectively captured the relationship between satellite data and in-situ turbidity across different ranges.

The analysis of the retrieved turbidity data revealed distinct spatiotemporal patterns along the river, with lower values during the dry season and significantly higher values during the flood season, peaking in September. The findings confirm that satellite remote sensing is a valuable tool for continuous, broad-scale monitoring of water quality, overcoming the spatial and temporal limitations of traditional, labor-intensive methods. It also supports informed decision-making for environmental protection and sustainable development, given the river's influence on the coastal ecosystems of the Gulf of Thailand. For future study, it is recommended to expand monitoring to the entire river basin to better understand spatio-temporal patterns. It is also recommended to explore alternative methods, such as semi-analytic or machine learning models, and to evaluate different atmospheric correction methods for use in clearer water bodies with low turbidity, such as lakes or oceans.

References

Acharya, T. D., Subedi, A., & Lee, D. H. (2018). Evaluation of water indices for surface water extraction in a Landsat 8 scene of Nepal. *Sensors*, *18*(8), Article No. 2580. https://doi.org/10.3390/s18082580

Allam, M., Meng, Q., Elhag, M., & et al. (2024). Atmospheric Correction Algorithms Assessment for Sentinel-2A Imagery over Inland Waters of China: Case Study, Qiandao Lake. *Earth System and Environment, 8*(1), 105–119. https://doi.org/10.1007/s41748-023-00366-w

Bidorn, B., Sok, K., Bidorn, K., & Burnett, W. C. (2021). An analysis of the factors responsible for the shoreline retreat of the Chao Phraya Delta (Thailand). *Science of The Total Environment*, *769*, 145253. https://doi.org/10.1016/j.scitotenv.2021.145253

Bilotta, G. S., & Brazier, R. E. (2008). Understanding the influence of suspended solids on water quality and aquatic biota. *Water Research*, *42*(12), 2849–2861. https://doi.org/10.1016/j.watres.2008.03.018

Borok, A. (2014). *Turbidity Technical Review: Summary of Sources, Effects, and Issues*

Related to Revising the Statewide Water Quality Standard for Turbidity. Oregon Department of Environmental Quality.

Cao, F., & Tzortziou, M. (2021). Capturing dissolved organic carbon dynamics with Landsat-8 and Sentinel-2 in tidally influenced wetland–estuarine systems. *Science of The Total Environment*, *777*, 145910. https://doi.org/10.1016/j.scitotenv.2021.145910

Cloern, J. E. (1987). Turbidity as a control on phytoplankton biomass and productivity in estuaries. *Continental Shelf Research*, *7*(11-12), 1367-1381. https://doi.org/10.1016/0278-4343(87)90042-2

Dogliotti, A. I., Ruddick, K. G., Nechad, B., Doxaran, D., & Knaeps, E. (2015). A single algorithm to retrieve turbidity from remotely-sensed data in all coastal and estuarine waters. *Remote Sensing of Environment*, *156*, 157-168. https://doi.org/10.1016/j.rse.2014.09.020

Elhag, M., Gitas, I., Othman, A., Bahrawi, J., & Gikas, P. (2019). Assessment of Water Quality Parameters Using Temporal Remote Sensing Spectral Reflectance in Arid Environments, Saudi Arabia. *Water*, *11*(3), 556. https://doi.org/10.3390/w11030556

Estes, L., Elsen, P. R., Treuer, T., Ahmed, L., Caylor, K., Chang, J., Choi, J. J., & Ellis, E. C. (2018). The spatial and temporal domains of modern ecology. *Nature Ecology & Evolution*, *2*, 819-826. https://doi.org/10.1038/s41559-018-0524-4

Gordon, H. R., Clark, D. K., Hovis, W. A., Austin, R. W., & Yentsch, C. S. (1985). Ocean color measurements. *Advances in Geophysics*, *27*, 297–333. https://doi.org/10.1016/S0065-2687(08)60408-2

Güttler, F. N., Niculescu, S., & Gohin, F. (2013). Turbidity retrieval and monitoring of Danube Delta waters using multi-sensor optical remote sensing data: An integrated view from the delta plain lakes to the western-northwestern Black Sea coastal zone. *Remote Sensing of Environment*, *132*, 86-101. https://doi.org/10.1016/j.rse.2013.01.009

Hydro and Agro Informatics Institute. (2012). *Data Warehouse System Development Project of 25 Basin and Flood and Drought Modeling* [In Thai].

Kolli, M. K., & Chinnasamy, P. (2024). Estimating turbidity concentrations in highly dynamic rivers using Sentinel-2 imagery in Google Earth Engine: Case study of the Godavari River, India. *Environmental Science and Pollution Research*, *31*, 33837–33847. https://doi.org/10.1007/s11356-024-33344-4

Kuhn, C., de Matos Valerio, A., Ward, N., Loken, L., Sawakuchi, H. O., Kampel, M., Richey, J., Stadler, P., Crawford, J., Striegl, R., Vermote, E., Pahlevan, N., & Butman, D. (2019). Performance of Landsat-8 and Sentinel-2 surface reflectance products for river remote sensing retrievals of chlorophyll-a and turbidity. *Remote Sensing of Environment*, *224*, 104-118. https://doi.org/10.1016/j.rse.2019.01.023

Liu, W., Wang, S., Yang, R., Ma, Y., Shen, M., You, Y., Hai, K., & Baqa, M. F. (2019). Remote Sensing Retrieval of Turbidity in Alpine Rivers based on high Spatial Resolution Satellites. *Remote Sensing*, *11*(24), 3010. https://doi.org/10.3390/rs11243010

Luo, Y., Doxaran, D., & Vanhellemont, Q. (2020). Retrieval and Validation of Water Turbidity at Metre-Scale Using Pléiades Satellite Data: A Case Study in the Gironde Estuary. *Remote Sensing*, *12*(6), 946. https://doi.org/10.3390/rs12060946

Marina, P., Snezana, M., Maja, N., & Miroslava, M. (2020). Determination of heavy metal concentration and correlation analysis of turbidity: A case study of the Zlot source (Bor, Serbia). *Water, Air, and Soil Pollution*, *231*(3), 1–12. https://doi.org/10.1007/s11270-020-

4453-x

Pahlevan, N., Mangin, A., Balasubramanian, S. V., Smith, B., & Warren, M. (2021). ACIXaqua: A global assessment of atmospheric correction methods for Landsat-8 and Sentinel-2 over lakes, rivers, and coastal waters. *Remote Sensing of Environment*, *258*, 112366. https://doi.org/10.1016/j.rse.2021.112366

Pimwiset, W., Tungkananuruk, K., Rungratanaubon, T., Kullavanijaya, P., & Veesommai Sillberg, C. (2022). Water Turbidity Determination by a Satellite Imagery-Based Mathematical Equation for the Chao Phraya River. *Environment and Natural Resources Journal*, *20*(3), 297–309. https://doi.org/10.32526/ennrj/20/202100237

Powers, S. M., Barnard, M. A., Macleod, M. S., Miller, L. A., & Wagner, N. D. (2023). Spatially intensive patterns of water clarity in reservoirs determined rapidly with sensor-equipped boats and satellites. *Journal of Geophysical Research: Biogeosciences*, *128*, e2023JG007650. https://doi.org/10.1029/2023JG007650

Richter, R. (1990). A fast atmospheric correction algorithm applied to Landsat TM images. *International Journal of Remote Sensing*, *11*(1), 159–166. https://doi.org/10.1080/01431169008955008

Ritchie, C. J., Zimba, P. V., & Everitt, H. J. (2003). Remote Sensing Techniques to Assess Water Quality. *Photogrammetric Engineering & Remote Sensing*, *69*(6), 695–704.

Shen, X., & Feng, Q. (2018). Statistical Model and Estimation of Inland Riverine Turbidity with Landsat 8 OLI Images: A Case Study. *Environmental Engineering Science*, *35*(2). https://doi.org/10.1089/ees.2016.054

Shrestha, M., Sampath, A., Kim, M., & Park, S. (2024). System characterization report on the Earth Surface Mineral Dust Source Investigation (EMIT) sensor. In S. N. R. Chandra (Comp.), *System characterization of Earth observation sensors* (U.S. Geological Survey Open-File Report 2021–1030, chap. R). U.S. Geological Survey. https://doi.org/10.3133/ofr20211030R

Suwanlertcharoen, T., Prukpitikul, S., & Buakaew, V. (2020). Retrieval of water turbidity using sentinel-2 image time series to enhance water quality assessment for consumption. *Journal of Environmental Management*, *16*, 74-93. https://doi.org/10.14456/jem.2020.12 [In Thai].

Suwanlertcharoen, T., Lawawirojwong, S., & Deeudomchan, K. (2024). Spatiotemporal distribution and occurrence of surface phytoplankton blooms using spectral indices derived from Sentinel-2 imagery in the Upper Gulf of Thailand. In *Proceedings of the 45th Asian Conference on Remote Sensing (ACRS)*. Asian Association on Remote Sensing.

Thompson, D. R., Green, R. O., Bradley, C., Brodrick, P. G., Mahowald, N., Dor, E. B., Bennett, M., Bernas, M., Carmon, N., Chadwick, K. D., Clark, R. N., Coleman, R. W., Cox, E., Diaz, E., Eastwood, M. L., Eckert, R., Ehlmann, B. L., Ginoux, P., Ageitos, M. G., Grant, K., Guanter, L., Pearlshtien, D. H., Helmlinger, M., Herzog, H., Hoefen, T., Huang, Y., Keebler, A., Kalashnikova, O., Keymeulen, D., Kokaly, R., Klose, M., Li, L., Lundeen, S. R., Meyer, J., Middleton, E., Miller, R. L., Mouroulis, P., Oaida, B., Obiso, V., Ochoa, F., Olson-Duvall, W., Okin, G. S., Painter, T. H., Pérez García-Pando, C., Pollock, R., Realmuto, V., Shaw, L., Sullivan, P., Swayze, G., Thingvold, E., Thorpe, A. K., Vannan, S., Villarreal, C., Ung, C., Wilson, D. W., & Zandbergen, S. (2024). On-orbit calibration and performance of the EMIT imaging spectrometer. *Remote Sensing of Environment*, *303*, 113986. https://doi.org/10.1016/j.rse.2023.113986

Topp, S. N., Pavelsky, T. M., Jensen, D., Simard, M., & Ross, M. R. V. (2020). Research Trends in the Use of Remote Sensing for Inland Water Quality Science: Moving Towards Multidisciplinary Applications. *Water*, *12*(1), 169. https://doi.org/10.3390/w12010169

Ulfa, K., Hendayani, Oktavia, M. I., Pradono, K. A., Fibriawati, L., Muchsin, F., Candra, D. S., & Damanik, K. W. V. (2020). Evaluation of atmospheric correction algorithms for Sentinel-2 over paddy field area. *IOP Conference Series: Earth and Environmental Science*, *500*, 012081. https://doi.org/10.1088/1755-1315/500/1/012081

Vanhellemont, Q. (2019a). Adaptation of the dark spectrum fitting atmospheric correction for aquatic applications of the Landsat and Sentinel-2 archives. *Remote Sensing of Environment*, *225*, 175–192. https://doi.org/10.1016/j.rse.2019.03.010

Vanhellemont, Q. (2019b). Daily metre-scale mapping of water turbidity using CubeSat imagery. *Optics Express*, *27*(20), A1372-A1399. https://doi.org/10.1364/OE.27.0A1372

Vanhellemont, Q. (2020). Sensitivity analysis of the dark spectrum fitting atmospheric correction for metre and decametre scale satellite imagery using autonomous hyperspectral radiometry. *Optics Express*, *28*(20), 29948–29965. https://doi.org/10.1364/OE.397456

Vanhellemont, Q., & Ruddick, K. (2014). Turbid wakes associated with offshore wind turbines observed with Landsat 8. *Remote Sensing of Environment*, *145*, 105–113. https://doi.org/10.1016/j.rse.2014.01.009

Vanhellemont, Q., & Ruddick, K. (2018). Atmospheric correction of metre-scale optical satellite data for inland and coastal water applications. *Remote Sensing of Environment*, *216*, 586-597. https://doi.org/10.1016/j.rse.2018.07.015

Virdis, S. G. P., Xue, W., Winijkul, E., Nitivattananon, V., & Punpukdee, P. (2022). Remote sensing of tropical riverine water quality using sentinel-2 MSI and field observations. *Ecological Indicators*, *144*, 109472. https://doi.org/10.1016/j.ecolind.2022.109472

Wang, D., Tang, B.-H., & Li, Z.-L. (2024). Evaluation of five atmospheric correction algorithms for multispectral remote sensing data over plateau lake. *Ecological Informatics, 82*, 102666. https://doi.org/10.1016/j.ecoinf.2024.102666

Warren, M. A., Simis, S. G., Martinez-Vicente, V., Poser, K., Bresciani, M., Alikas, K., Spyrakos, E., Giardino, C., & Ansper, A. (2019). Assessment of atmospheric correction algorithms for the Sentinel-2A MultiSpectral Imager over coastal and inland waters. *Remote Sensing of Environment*, *225*, 267–289. https://doi.org/10.1016/j.rse.2019.03.018

Wu, J., Chen, P., Fu, S., Chen, Q., & Pan, X. (2023). Co-inversion of island leaf area index combination morphological and spectral parameters based on UAV multi-source remote sensing data. *Ecological Informatics*, *77*, 102190. https://doi.org/10.1016/j.ecoinf.2023.102190

Xu, Y., Feng, L., Zhao, D., & Lu, J. (2020). Assessment of Landsat atmospheric correction methods for water color applications using global AERONET-OC data. *International Journal of Applied Earth Observation and Geoinformation*, *93*, 102192. https://doi.org/10.1016/j.jag.2020.102192

Yuan, L. L. (2021). Continental-scale effects of phytoplankton and non-phytoplankton turbidity on macrophyte occurrence in shallow lakes. *Aquatic Sciences*, *83*(1), 14. https://doi.org/10.1007/s00027-020-00769-1